Journal of Medical Imaging & Case Reports

https://doi.org/10.17756/micr.2024-102

Case Report

Open Access

# Fibroblast Activation Protein Identifies Progressive Bladder Cancer and Allows Peritoneal Metastasis Detection by $^{68}$Ga-FAPI PET/CT Imaging – A Case Report

**Bastiaan J. Viergever[1,2], Esther Strating[1,2], Marnix Lam[3], Onno Kranenburg[1,4] and Richard P. Meijer[1,2*]**

[1]*Laboratory Translational Oncology, University Medical Center Utrecht, Utrecht, The Netherlands*

[2]*Department of Oncological Urology, University Medical Center Utrecht, Utrecht, The Netherlands*

[3]*Department of Radiology, University Medical Center Utrecht, Utrecht, The Netherlands*

[4]*Utrecht Platform for Organoid Technology, Utrecht, The Netherlands*

***Correspondence to:**
Richard P. Meijer
Laboratory Translational Oncology,
University Medical Center Utrecht,
Utrecht, The Netherlands.

Department of Oncological Urology,
University Medical Center Utrecht,
Utrecht, The Netherlands.
**E-mail:** rmeijer6@umcutrecht.nl

**Received:** October 23, 2023
**Accepted:** March 22, 2024
**Published:** March 27, 2024

**Citation:** Viergever BJ, Strating E, Lam M, Kranenburg O, Meijer RP. 2024. Fibroblast Activation Protein Identifies Progressive Bladder Cancer and Allows Peritoneal Metastasis Detection by $^{68}$Ga-FAPI PET/CT Imaging – A Case Report. *J Med Imaging Case Rep* 8(1): 5-11.

**Copyright:** © 2024 Viergever et al. This is an Open Access article distributed under the terms of the Creative Commons Attribution 4.0 International License (CCBY) (http://creativecommons.org/licenses/by/4.0/) which permits commercial use, including reproduction, adaptation, and distribution of the article provided the original author and source are credited.

Published by United Scientific Group

## Abstract

**Objective:** Currently, [$^{18}$F] FDG-PET/CT scans are used in advanced bladder cancer patients to identify metastatic lesions. Unfortunately, FDG-PET/CT displays relatively low sensitivity in detecting metastatic disease in these patients, resulting in open-and-close operations due to unexpected metastatic disease. Recently a novel radiotracer has emerged using FAP targeting [$^{68}$Ga] FAPI-46, raising the question if this provides a more accurate alternative to [$^{18}$F] FDG-PET/CT for detecting metastatic lesions in bladder cancer patients.

**Methodology:** FAP expression was assessed in primary and metastatic samples of two patients with MIBC using immunohistochemical analysis. Finally, both FDG and FAPI scans were obtained and compared using [$^{18}$F] FDG-PET/CT and [$^{68}$Ga] FAPI-46-PET/CT.

**Results:** FAP protein expression was found to be high in both primary and metastatic tumor lesions. In the primary tumor lesions, FAP expression was mainly observed in the fibrotic area adjacent to the tumor bulk. In contrast, PM showed FAP expression closely surrounding small tumor clusters. Finally, metastatic lesions that were undetectable on [$^{18}$F] FDG-PET/CT were detected using [$^{68}$Ga] FAPI-46-PET/CT. FAPI-46-PET/CT findings of PM correlated with lesions found in the open-and-close surgical procedures.

**Conclusion:** [$^{68}$Ga] FAPI-46-PET/CT offers a promising additional tool to [$^{18}$F] FDG-PET/CT for identifying peritoneal metastatic lesions of bladder cancer in high-risk patients.

## Keywords

Bladder cancer, Molecular imaging, Metastases, Molecular subtypes, Fibroblast activation protein, Positron emission tomography

## List of Abbreviations

[$^{18}$F] FDG is Fluor-18 2-fluoro-2-deoxy-D-glucose; FAP is Fibroblast Activation Protein; $^{68}$Ga-FAPI PET/CT is Gallium-68 Fibroblast Activation Protein PET/CT Imaging; FDG-PET/CT is Fluorodeoxyglucose Positron Emission Tomography/Computed Tomography; NMIBC is Non-Muscle Invasive Bladder Cancer; MIBC is Muscle Invasive Bladder Cancer; PM is Peritoneal Metastases; TME is Tumor Microenvironment; PET is Positron Emission Tomography; UMCU is University Medical Center Utrecht; CK5 is Keratin 5; CK20 is Keratin 20; TP53 is Tumor Protein 53; TP63 is Tumor Protein 63; H&E is Hematoxylin & Eosin; PALGA is Pathologisch Anatomisch

Landelijk Geautomatiseerd Archief (Dutch pathology database); and IKNL is Integraal Kankercentrum Nederland (Comprehensive Cancer Centre Netherlands).

## Introduction

Bladder cancer ranks amongst the top five and top ten of most common cancers worldwide in men and women, respectively [1]. Over 6,755 patients were diagnosed with bladder cancer in the Netherlands in 2022 [2], consisting of NMIBC (73% of total) or MIBC/metastatic disease [3-5]. In general, NMIBC has a high recurrence rate (up to 84%), but rarely metastasizes, whereas MIBC is an aggressive disease with a high risk for relapse and metastases (up to 50%) [4, 5]. In 2021, nearly 350 patients were diagnosed with metastatic bladder cancer in the Netherlands [2]. Patients that are at risk of metastatic disease can be checked with the standard of care PET scan using [$^{18}$F] FDG-PET/CT PET tracer [6, 7]. Though providing a non-invasive method to detect metastatic bladder cancer, the [$^{18}$F] FDG tracer only has a sensitivity range between 54 to 87% for detecting distant metastases of bladder cancer [8-12]. This results in patients with difficult to image metastases [13], such as PM being diagnosed with a lower degree of disease than is actually present and thus increases difficulty in first time-right treatment installation (e.g., neoadjuvant chemotherapy prior to definitive local therapy).

In recent years whole genome expression and sequencing studies have identified key genes and pathways in the development of urothelial bladder cancer (e.g., TP53, RB1, E2F3, FGFR3, CDKN2A, and Stag2) [14-16], which may also be involved in disease progression, response to chemotherapy and resistance development [17-19]. Furthermore, recent studies have shown that the TME plays a key role in treatment responses, disease progression and overall survival chances of patients in several cancer types, among which bladder cancer [20-22]. Recently, it was shown that the TME and more specifically FAP was found as a predictive marker for CMS4-subtype of colorectal cancer, especially for PMs. Furthermore, targeting FAP with [$^{68}$Ga]-FAPI-46 as PET/CT tracer allowed non-invasive molecular imaging using [$^{68}$Ga] FAPI-46-PET/CT imaging [23, 24]. Recently, the potential of [$^{68}$Ga] FAPI-46-PET/CT was first reported for bladder cancer [25]. Application of FAPI-PET/CT in both bladder cancer and other tumor types have yielded promising results in detecting lesions often missed using golden standard glucose-based radiotracers [25-28].

Here, we present two patient cases where we evaluate FAP as predictive marker for PM disease of bladder cancer by both immunohistochemical analysis and [$^{68}$Ga] FAPI-46 tracer in direct comparison to [$^{18}$F] FDG-PET/CT. Based on these findings, we provide this case report illustrating the prognostic value of [$^{68}$Ga] FAPI-46-PET/CT for peritoneal metastasized bladder cancer.

## Case Report

### Patient selection

The patient was referred for a [$^{68}$Ga] FAPI-46-PET/CT by the oncologist who at that time faced a diagnostic challenge that could not be solved with standard diagnostic imaging. These patients were presented with advanced metastatic disease that was not detected using [$^{18}$F] FDG-PET/CT, resulting in the tumor lesions being detected at the scheduled curative surgical resection of disease. Curative resection was not possible and thus discontinued, however PM biopsies were resected for histopathological conformation. In total, 2 patients were included in 2023 in the UMCU that presented a diagnostic challenge that could not be solved using standard diagnostic imaging.

### Immunohistochemistry

Transurethral bladder tumor-tissue and surgically resected metastatic tumor-samples from both patients were fixed in 4% paraformaldehyde for 1 to 6 h, dehydrated, and paraffin-embedded according to standard histology procedures. Sections were stained with H&E or the following primary antibodies: CK5 (Abcam, ab52635), CK20 (DakoCytomation, M7019), Ki67 (Dako, M7240), TP53 (Santa Cruz, sc-126), TP63 (Abcam, ab735), panCytokeratin 1/3 (CKAE1/3, Pierce Antibodys, MA5-13156) and anti-FAP (Abcam, ab207178), were stained according to the manufacturer's protocols. All staining's were performed in tandem with healthy control tissues as positive, negative, and healthy bladder controls, as previously reported in [29, 30]. The following secondary antibodies conjugated with HRP were used: bright vision poly-HRP-anti rabbit IgG (VWR international, VWRKDPVR110HRP) and poly-HRP-anti-mouse IgG (VWR international, VWRKDPVM110HRP) for 1 h at room temperature, and Goat IgG HRP-conjugated antibody (R&D Systems Europe, HAF017) for 1 h at 37 °C. Staining was performed using 3,3'-diaminobenzidine for 10 min exactly at room temperature. Images were acquired by slide scanning and analyzed using the NDP.view (v2.7.39) software (Hamamatsu Photonics K.K.).

### [$^{68}$Ga] FAPI-46-PET/CT clinical production, quality control and imaging

FAPI-46 precursor for labeling was supplied by SOFIE Biosciences (Totowa, NJ, USA), ascorbic acid was obtained from Polatom (Otwoch, Poland). [$^{68}$Ga] FAPI-46-PET/CT imaging, quality control, clinical production was performed as preciously described [23]. After obtaining the patient's informed consent PET/CT images were made one hour after intra-venous injection of [$^{68}$Ga]-DOTA-FAPI-46 at 1.5 MBq/kg injected dose.

## Results

### Study population

Two patients with MIBC were included in this study; Patient #1 was a woman with a suspected cT1G3N0M0 urothelial carcinoma with carcinoma *in situ* based on cytoscopic evaluation and biopsies (Figure 1a). Patient #2 was a man that was included with a suspected cT2-3G3N0M0 urothelial carcinoma with carcinoma *in situ* based on cytoscopic evaluation and biopsies (Figure 2a). Both primary

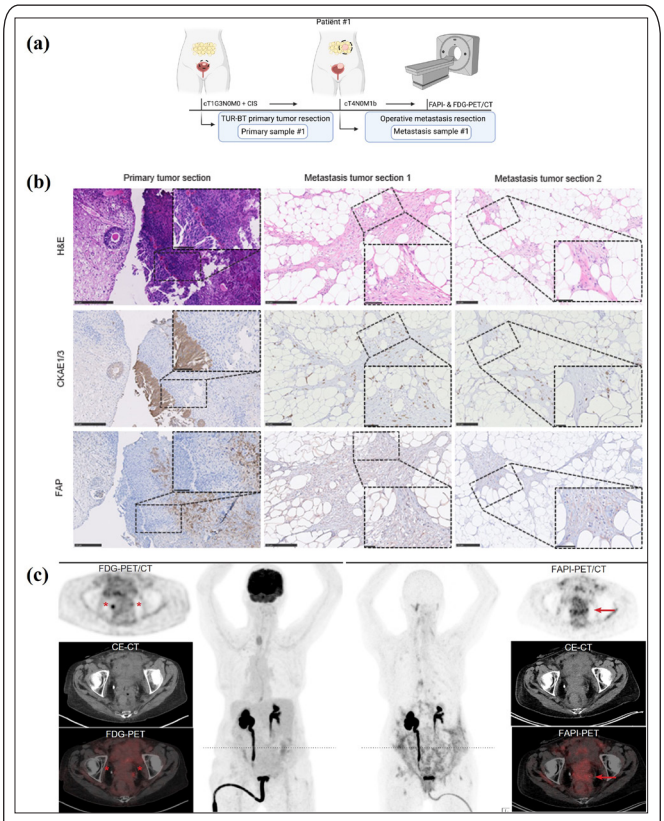


**Figure 1:** Patient 1 immunohistochemical FAP and FAPI-PET/CT analysis. **(a)** Overview of clinical timeline of patient 1 with respective sampling and scanning moments indicated. **(b)** Immunohistochemical analysis of patient 1 displayed with H&E and their expression of panCytokeratin (CKAE1/3) and FAP. Tumor sections are from the black box indicated sections from the respective supplemental figure 2 and figure 3 H&E complete slides, with scale bars are 500 µm for all tumor sections. The zooms indicated by dotted boxes are displayed with respective scalebars of 100 µm. and **(c)** Side by side [$^{18}$F] FDG-PET/CT and [$^{68}$Ga] FAPI-46-PET/CT scans of patient 1 with their respective tracer activity. Physiological [$^{18}$F] FDG activity in both ureters (red asterisk) and [$^{68}$Ga] FAPI-46 activity in cavum Douglasi (red arrow). The dotted line indicates the transversal plane of the side images.

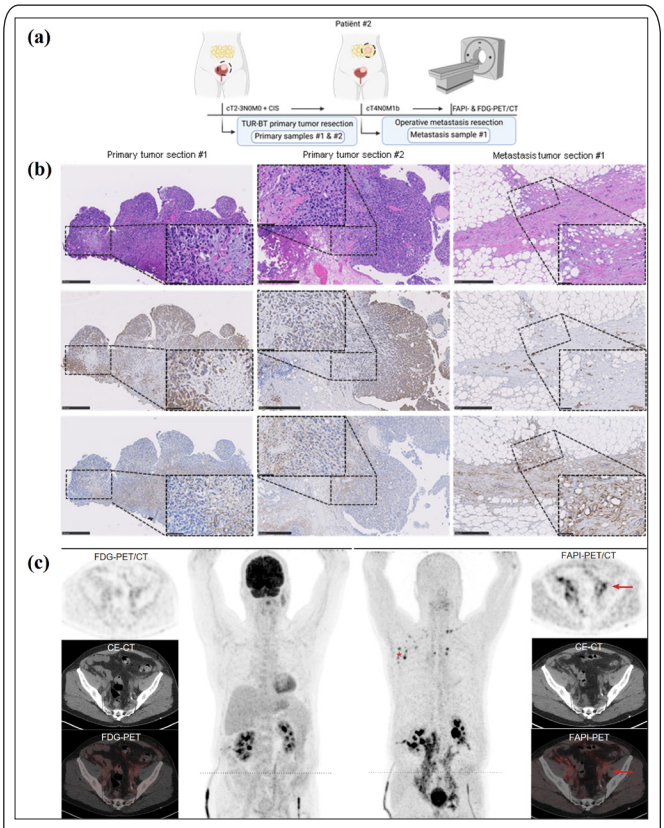


**Figure 2:** Patient 2 immunohistochemical FAP and FAPI-PET/CT analysis. **(a)** Overview of clinical timeline of patient 2 with respective sampling and scanning moments indicated. **(b)** Immunohistochemical analysis of patient 1 displayed with H&E and their expression of panCytokeratin (CKAE1/3) and FAP. Tumor sections are from black box indicated sections from the respective supplemental figure 4 and figure 5 H&E complete slides, with scale bars are 500 µm for all tumor sections. The zooms indicated by dotted boxes are displayed with respective scalebars of 100 µm. and **(c)** Side by side [$^{18}$F] FDG-PET/CT and [$^{68}$Ga] FAPI-46-PET/CT scans of patient 2 with their respective tracer activity. Pathological [$^{68}$Ga] FAPI-46 activity in around left ureter and (retro)peritoneal (red arrow). The dotted line indicates the transversal plane of the side images.

tumors were sampled in their respective peripheral hospitals in the first presentation during the cytoscopic evaluation. Both patients were transferred to the UMCU for a radical cystectomy. They were screened for metastatic disease with [$^{18}$F] FDG-PET/CT, which showed no distant metastasis. At the start of the cystectomy procedure, both patients had multiple metastatic peritoneal lesions that were not detected using the [$^{18}$F] FDG-PET/CT. A curative surgical resection of disease was not possible; however, PM biopsies were resected for histopathological conformation.

## Tumor-selective expression of FAP in tumor fibrotic area adjacent to cancer cells in primary tumor and surrounding PM clusters of patient 1

The primary tumor lesion and peritoneal metastases of patient 1 (Figure 1a) were analyzed using immunohistochemical analysis (Figure 1b). Tumor sections were identified using H&E and panCytokeratin 1/3 (CKAE1/3). Evaluating the FAP expression within the section, high levels of FAP expression were found in the fibrotic area adjacent to the tumor bulk mass in the primary tissue. This has previously been described in primary NMBIC [21], being characteristic to the activation and recruitment of fibroblasts to the border of tumor. FAP expression of metastatic section zooms #1 and #2 were found to be closely surrounded by small individual tumor clusters (Figure 1b), with overall high levels of FAP expression within the peritoneal tumor slide. Compared to healthy bladder control tissue (Supplemental figure 1), tumor proliferative Ki67 and subtype markers CK5, CK20, TP53 and TP63 were found to be heterogeneously expressed within the primary tumor sections (Supplemental figure 2). PM section zooms #1 and #2 of patient 1 show less variation in marker expression than the primary tumor (Supplemental figure 3), with metastatic lesions predominantly being TP53 and CK20 positive and TP63 and CK5 negative, indicative of more p53-like subtype [16]. Taken together, this provides confirmation of the histopathological FAP expression in the primary tumor and PM lesion of patient 1.

## FAPI-PET/CT detects PM of patient 1

After the open-and-close surgical procedure, patient 1 was scanned with both [$^{68}$Ga] FAPI-46-PET/CT and [$^{18}$F] FDG-PET/CT within an 18-day timeframe (Figure 1a and

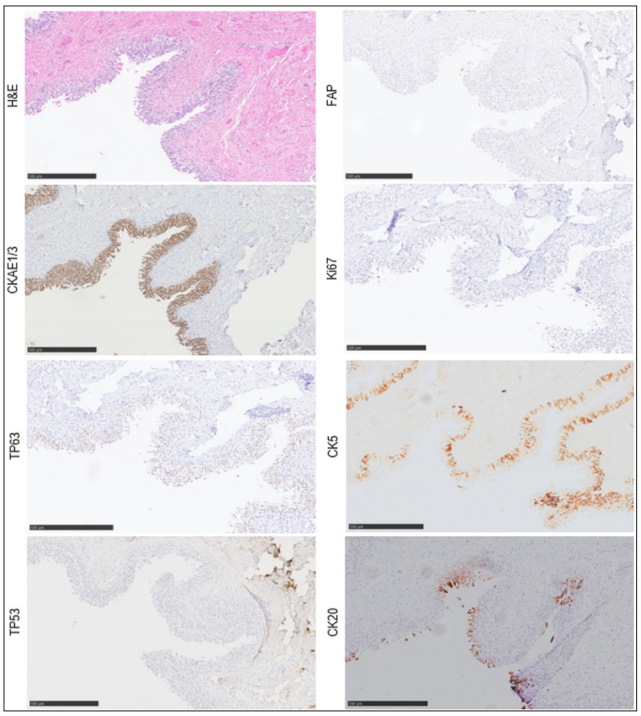


**Supplemental Figure 1:** Immunohistochemistry controls on healthy bladder tissue. Immunohistochemical analysis of patient 1 displayed with H&E and their expression of Ki67, TP53, TP63, CK5, and CK20. Scale bars with are 500 µm.

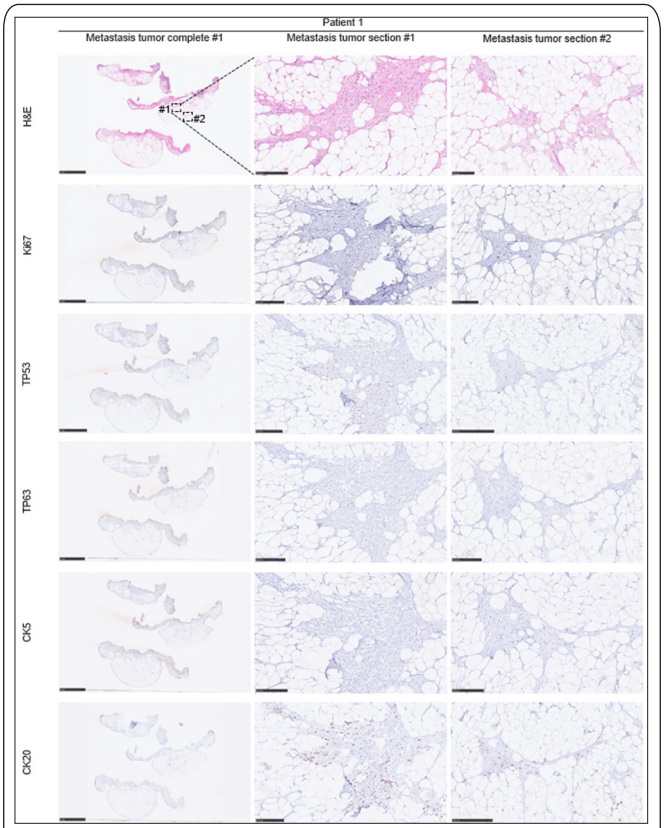


**Supplemental Figure 3:** Patient 1 immunohistochemical analysis of peritoneal metastasis sample #1. Immunohistochemical analysis of patient 1 displayed with H&E and their expression of Ki67, TP53, TP63, CK5, and CK20. Scale bars of complete scans are 5 mm. Tumor section zooms are indicated in the complete H&E slide with #1 and #2 respectively, with tumor section scale bars of 500 µm.

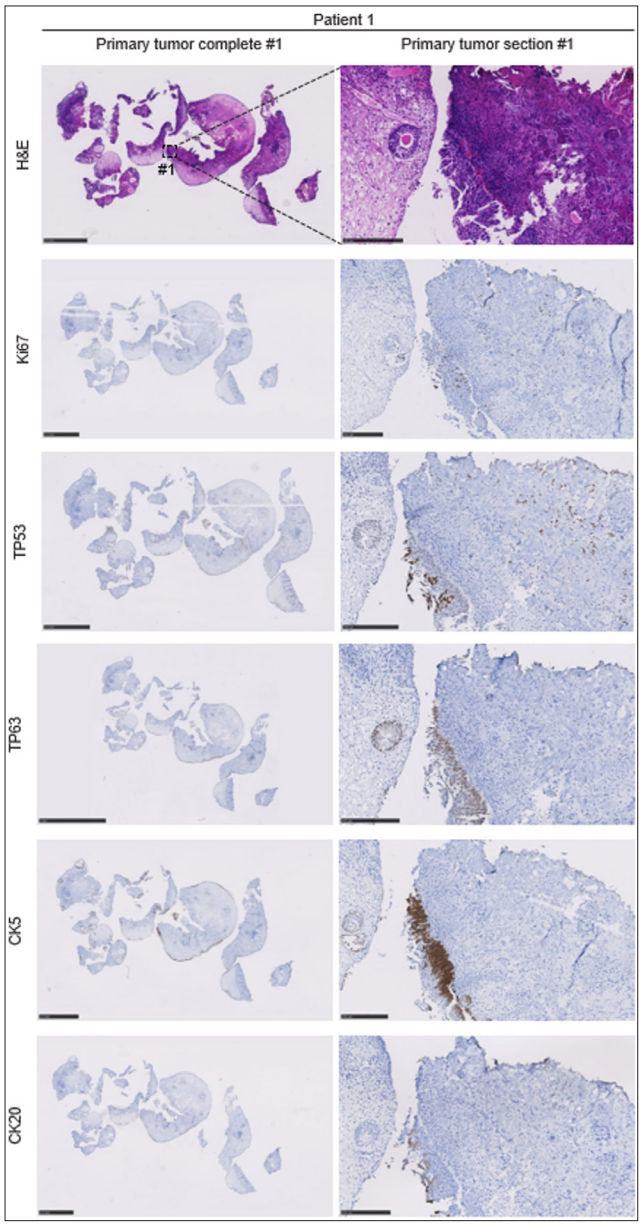


**Supplemental Figure 2:** Patient 1 immunohistochemical analysis of primary tumor sample #1. Immunohistochemical analysis of patient 1 displayed with H&E and their expression of Ki67, TP53, TP63, CK5, and CK20. Scale bars of complete scans are 5 mm. Tumor section zooms are indicated in the respective complete H&E slide with #1, with tumor section scale bars of 500 µm.

1c). There was little to no activity on the FDG-PET/CT. Physiological [$^{18}$F] FDG activity was seen in both ureters (red asterisk). The [$^{68}$Ga] FAPI-46-PET/CT showed intense activity in the peritoneum at the level of cavum Douglasi (Figure 1c, red arrow) which corresponded to the PM found during the surgical procedure.

## Tumor-selective expression of FAP in tumor fibrotic area adjacent and within tumor bulk of primary tumor and surrounding PM clusters in patient 2

Primary tumor lesions of patient 2 in combination with PM sample (Figure 2a) were analyzed using immunohistochemical analysis (Figure 2b). Tumor sections were identified using the H&E and CKAE1/3. Similar to patient 1, FAP expression

within the sections are high in the fibrotic area adjacent to the tumor bulk mass in the primary tissue (Zoom of section #1 and #2). Interestingly, stromal infiltration of the tumor bulk is also seen (Zoom of section #1 and #2). The FAP expression of the metastatic section zooms #1 and #2 were similar to patient 1, with high FAP expression closely surrounding small individual tumor clusters (Figure 2b). Compared to the control healthy bladder tissues (Supplemental figure 1), tumor proliferative Ki67 and subtype markers CK5, CK20, TP53 and TP63 were found to be heterogeneous within the primary tumor sections (Supplemental figure 4) in both the complete tumor slides #1 and #2. Corresponding with the PM of patient 1, PM section #1 and zoom #1 of patient 2 show less variation in marker expression than the primary tumor (Supplemental figure 5). Interestingly, PM lesions of patient 2 were predominantly TP53 and TP63 positive and CK5 and CK20 negative, indicating more urobasal A subtype [31]. Similar to the PM lesion of patient 1, this shows similar histopathological FAP expression in the primary and PM tumor lesions of patient 2.

### FAPI-PET/CT detects PM in patient 2

After the open-and-close surgical procedure, patient 2 was scanned with both [$^{68}$Ga] FAPI-46-PET/CT and [$^{18}$F] FDG-PET/CT within a 3-day timeframe (Figure 2a and 2c). Again, there was little to no activity on the FDG-PET/CT. The patient showed higher FAPI-PET/CT activity with pathological [$^{68}$Ga] DOTA-FAPI-46 activity in around left ureter and (retro)peritoneum (Figure 2c, red arrow), similar to the lesions seen at the open-and-close surgical procedure. A specific uptake in supradiaphragmatic lymph nodes is highlighted with the red asterisk.

## Discussion

In this case report, we present two patients diagnosed with peritoneal metastatic bladder cancer during an open-and-close procedure. These peritoneal lesions were undetected by [$^{18}$F] FDG-PET/CT but identified using [$^{68}$Ga] FAPI-46-PET/CT. Although efforts were made to minimize the time gap between FDG- and FAPI-PET/CT scans, there were

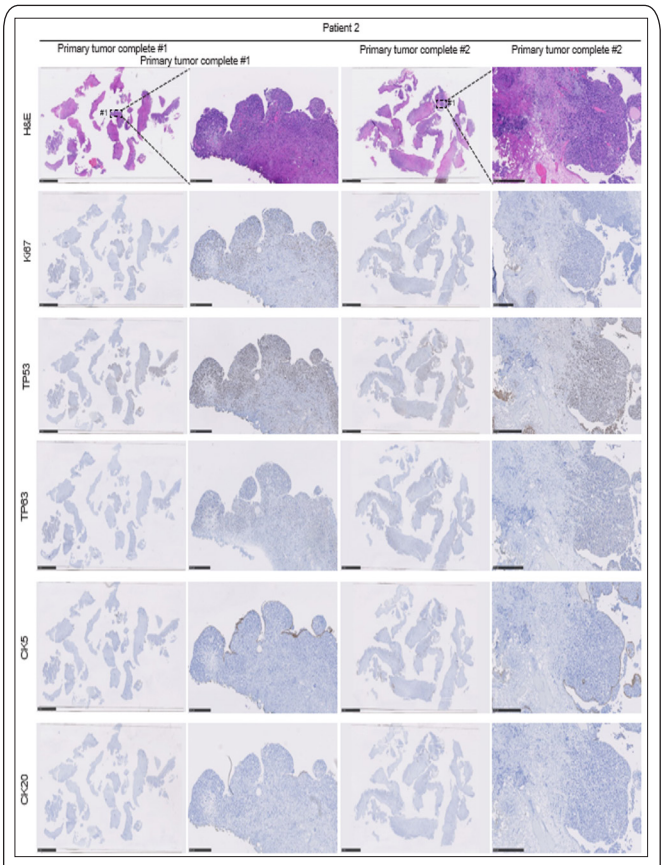


**Supplemental Figure 4:** Patient 2 immunohistochemical analysis of primary tumor samples #1 and #2. Immunohistochemical analysis of patient 2 displayed with H&E and their expression of Ki67, TP53, TP63, CK5, and CK20. Scale bars of complete scans are 5 mm. Tumor section zooms are indicated in the respective complete H&E slide with #1, with tumor section scale bars of 500 µm.

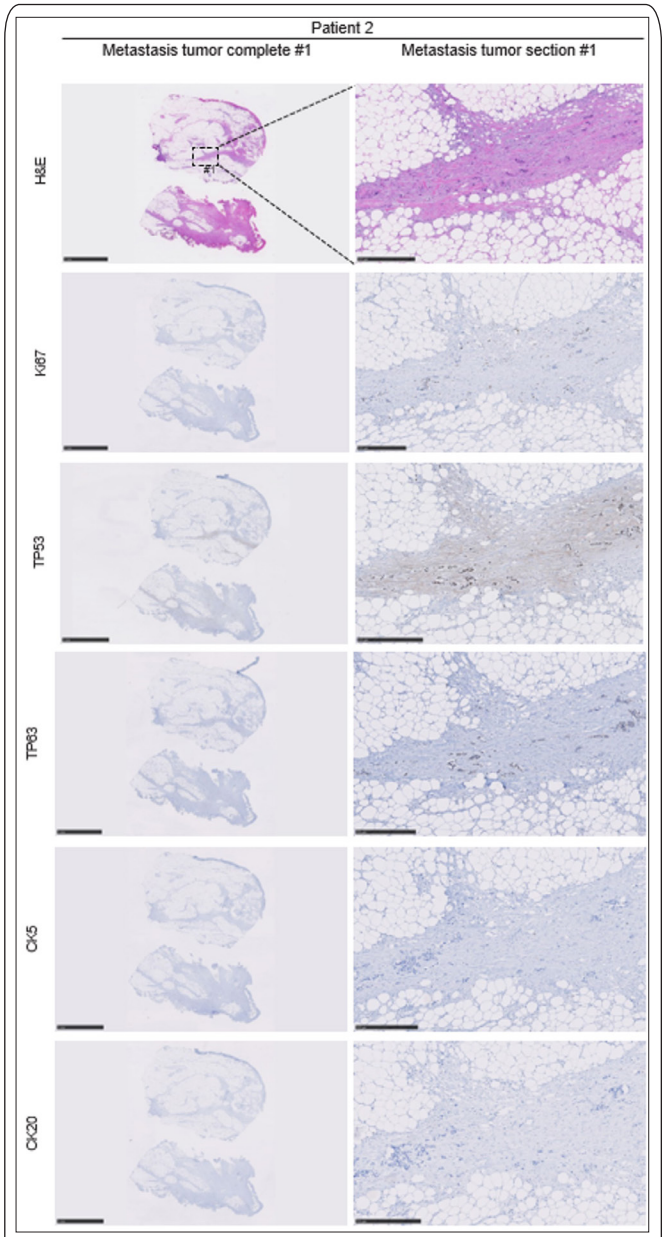


**Supplemental Figure 5:** Patient 2 immunohistochemical analysis of peritoneal metastasis sample #1. Immunohistochemical analysis of patient 1 displayed with H&E and their expression of Ki67, TP53, TP63, CK5, and CK20. Scale bars of complete scans are 5 mm. Tumor section zooms are indicated in the complete H&E slide with #1 respectively, with tumor section scale bars of 500 µm.

instances of a several-day interval between the scans. However, this temporal disparity is unlikely to account for the large differences in activities observed between FDG- and FAPI-PET/CT scans. The possibility of missing lesions due to tissue specific small or even absent stromal tissue around tumor lesions is to be expected and warrants further investigation in future studies to the percentage of missed lesions. Additionally, we provide a direct comparison of primary and metastatic tissue for common bladder cancer markers and FAP. Immunohistochemical analysis confirmed high FAP expression in both primary and peritoneal metastatic lesions. The authors would like to emphasize that this case report has its limitations due to a cohort size of only two patients. This limitation is mainly affecting the possibility to generalize results and extrapolate findings to the bladder cancer population. Furthermore, only [$^{68}$Ga] FAPI-46-PET/CT was used, results may vary using other isotopes. Additionally, local disease was difficult to assess in both FDG- and FAPI-PET/CT due to renal clearing of the markers, limiting diagnostic possibilities for localized disease. Advantages and disadvantages of FAPI-PET/CT over FDG-PET/CT for localized disease should be further assessed using delayed nuclear imaging after renal clearing, also known as delayed-time-point scanning [32]. Therefore, we suggest that these results and suggestions should be confirmed in future research projects with a larger study population.

## Conclusion

Here, we directly compare immunohistochemical expression of FAP in primary and PM lesions to results from molecular imaging using the current standard of care [$^{18}$F] FDG-PET/CT and [$^{68}$Ga] FAPI-46-PET/CT activity in two patients. We find high expression of FAP protein in both primary tumor lesions in the fibrotic area adjacent to the tumor bulk. Furthermore, we see high FAP expression surrounding tumor cell clusters in the PM of these patients. Finally, a clear increase was seen of [$^{68}$Ga] DOTA-FAPI-46 in the abdomen and peritoneal regions of these patients, where [$^{18}$F] FDG shows little to no signal compared to the background. These findings mimic results found in PM of colorectal cancer. Though the study population in this case-report is limited, the results of this study highlight the possibilities of [$^{68}$Ga] FAPI-46-PET/CT to identify metastases in bladder cancer patients that are missed using the golden standard [$^{18}$F] FDG-PET/CT. Future studies using larger cohort sizes should endeavor to further study the added benefits of using FAPI-46-PET/CT, alternative isotype variant and even the possibility of targeting bladder cancer tumors using theragnostic application of FAPI-46-PET/CT for metastatic bladder cancer and local diseases. Overall, we show that FAP and its use as PET tracer as [$^{68}$Ga] DOTA-FAPI-46 are an accurate and highly potential additional tool to the standard of care [$^{18}$F] FDG-PET/CT scan for identifying metastatic lesions in advanced bladder cancer patients.

## Acknowledgements

FAPI was kindly provided by SOFIE Biosciences. The authors would like to thank the Pathologisch Anatomisch Landelijk Geautomatiseerd Archief (PALGA), the Meander Medical Center and the Tergooi Medical Center in the transfer of FFPE material.

## Conflict of Interest

None.

## Ethics Approval and Consent

In accordance with UMC Utrecht values, EU data protection law, and according to Dutch laws and regulations patient consent was obtained for the use of patient material and images in this publication and may be the subject of a press release and may be linked to social media and/or used in other promotional activities. The study was performed in accordance with the Declaration of Helsinki.

### References

1. Siegel RL, Miller KD, Fuchs HE, Jemal A. 2021. Cancer statistics, 2021. *CA Cancer J Clin* 71(1): 7-33. https://doi.org/10.3322/caac.21654
2. Incidence of Bladder Cancer. [https://iknl.nl/kankersoorten/blaaskanker/registratie/incidentie] [Accessed March 27, 2024]
3. Chen C, Hu L, Chen Y, Hou J. 2017. The prognostic value of histological subtype in patients with metastatic bladder cancer. *Oncotarget* 8(17): 28408-28417. https://doi.org/10.18632/oncotarget.16083
4. Witjes JA, Bruins HM, Cathomas R, Compérat EM, Cowan NC, et al. 2021. European Association of Urology guidelines on muscle-invasive and metastatic bladder cancer: summary of the 2020 guidelines. *Eur Urol* 79(1): 82-104. https://doi.org/10.1016/j.eururo.2020.03.055
5. Babjuk M, Burger M, Capoun O, Cohen D, Compérat EM, et al. 2022. European Association of Urology guidelines on non–muscle-invasive bladder cancer (Ta, T1, and carcinoma *in situ*). *Eur Urol* 81(1): 75-94. https://doi.org/10.1016/j.eururo.2021.08.010
6. Yoon HJ, Yoo J, Kim Y, Lee DH, Kim BS. 2017. Enhanced application of 18F-FDG PET/CT in bladder cancer by adding early dynamic acquisition to a standard delayed PET protocol. *Clin Nucl Med* 42(10): 749-755. https://doi.org/10.1097/RLU.0000000000001780
7. Higashiyama A, Komori T, Juri H, Inada Y, Azuma H, et al. 2018. Detectability of residual invasive bladder cancer in delayed $^{18}$F-FDG PET imaging with oral hydration using 500 mL of water and voiding-refilling. *Ann Nucl Med* 32: 561-567. https://doi.org/10.1007/s12149-018-1280-x
8. Apolo AB, Riches J, Schöder H, Akin O, Trout A, et al. 2010. Clinical value of fluorine-18 2-fluoro-2-deoxy-D-glucose positron emission tomography/computed tomography in bladder cancer. *J Clin Oncol* 28(25): 3973-3978. https://doi.org/10.1200/JCO.2010.28.7052
9. Öztürk H. 2015. Detecting metastatic bladder cancer using $^{18}$F-fluorodeoxyglucose positron-emission tomography/computed tomography. *Cancer Res Treat* 47(4): 834-843. https://doi.org/10.4143/crt.2014.157
10. Goodfellow H, Viney Z, Hughes P, Rankin S, Rottenberg G, et al. 2014. Role of fluorodeoxyglucose positron emission tomography (FDG PET)-computed tomography (CT) in the staging of bladder cancer. *BJU Int* 114(3): 389-395. https://doi.org/10.1111/bju.12608
11. Yang Z, Cheng J, Pan L, Hu S, Xu J, et al. 2012. Is whole-body fluorine-18 fluorodeoxyglucose PET/CT plus additional pelvic images (oral hydration–voiding–refilling) useful for detecting recurrent bladder cancer? *Ann Nucl Med* 26: 571-577. https://doi.org/10.1007/s12149-012-0614-3
12. Girard A, Vila Reyes H, Shaish H, Grellier JF, Dercle L, et al. 2020. The role of 18F-FDG PET/CT in guiding precision medicine for invasive bladder carcinoma. *Front Oncol* 10: 565086. https://doi.org/10.3389/fonc.2020.565086

13. Healy JC. 2001. Detection of peritoneal metastases. *Cancer Imaging* 1: 4-12. https://doi.org/10.1102/1470-7330.2001.002
14. The Cancer Genome Atlas Research Network. 2014. Comprehensive molecular characterization of gastric adenocarcinoma. *Nature* 513: 202-209. https://doi.org/10.1038/nature13480
15. Daher A, de Boer WI, Le Frère-Belda MA, Kheuang L, Abbou CC, et al. 2004. Growth, differentiation and senescence of normal human urothelium in an organ-like culture. *Eur Urol* 45(6): 799-805. https://doi.org/10.1016/j.eururo.2004.01.002
16. Knowles MA, Hurst CD. 2015. Molecular biology of bladder cancer: new insights into pathogenesis and clinical diversity. *Nat Rev Cancer* 15(1): 25-41. https://doi.org/10.1038/nrc3817
17. Choi W, Czerniak B, Ochoa A, Su X, Siefker-Radtke A, et al. 2014. Intrinsic basal and luminal subtypes of muscle-invasive bladder cancer. *Nat Rev Urol* 11(7): 400-410. https://doi.org/10.1038/nrurol.2014.129
18. Kakehi Y, Özdemir E, Habuchi T, Yamabe H, Hashimura T, et al. 1998. Absence of p53 overexpression and favorable response to cisplatin-based neoadjuvant chemotherapy in urothelial carcinomas. *Jpn J Cancer Res* 89(2): 214-220. https://doi.org/10.1111/j.1349-7006.1998.tb00551.x
19. Sarkis AS, Bajorin DF, Reuter VE, Herr HW, Netto G, et al. 1995. Prognostic value of p53 nuclear overexpression in patients with invasive bladder cancer treated with neoadjuvant MVAC. *J Clin Oncol* 13(6): 1384-1390. https://doi.org/10.1200/JCO.1995.13.6.1384
20. Sounni NE, Noel A. 2013. Targeting the tumor microenvironment for cancer therapy. *Clin Chem* 59(1): 85-93. https://doi.org/10.1373/clinchem.2012.185363
21. Muilwijk T, Akand M, Daelemans S, Marien K, Waumans Y, et al. 2021. Stromal marker fibroblast activation protein drives outcome in T1 non-muscle invasive bladder cancer. *PLoS One* 16(9): 1-9. https://doi.org/10.1371/journal.pone.0257195
22. Goulet CR, Champagne A, Bernard G, Vandal D, Chabaud S, et al. 2019. Cancer-associated fibroblasts induce epithelial–mesenchymal transition of bladder cancer cells through paracrine IL-6 signalling. *BMC Cancer* 19: 1-13. https://doi.org/10.1186/s12885-019-5353-6
23. Strating E, Wassenaar E, Verhagen M, Rauwerdink P, van Schelven S, et al. 2022. Fibroblast activation protein identifies consensus molecular subtype 4 in colorectal cancer and allows its detection by $^{68}$Ga-FAPI-PET imaging. *Br J Cancer* 127(1): 145-155. https://doi.org/10.1038/s41416-022-01748-z
24. Altmann A, Haberkorn U, Siveke J. 2021. The latest developments in imaging of fibroblast activation protein. *J Nucl Med* 62(2): 160-167. https://doi.org/10.2967/jnumed.120.244806
25. Novruzov E, Dendl K, Ndlovu H, Choyke PL, Dabir M, et al. 2022. Head-to-head intra-individual comparison of [$^{68}$Ga]-FAPI and [$^{18}$F]-FDG PET/CT in patients with bladder cancer. *Mol Imaging Biol* 24(4): 651-658. https://doi.org/10.1007/s11307-022-01715-3
26. Koerber SA, Röhrich M, Walkenbach L, Liermann J, Choyke PL, et al. 2023. Impact of $^{68}$Ga-FAPI PET/CT on staging and oncologic management in a cohort of 226 patients with various cancers. *J Nucl Med* 64(11): 1712-1720. https://doi.org/10.2967/jnumed.123.266046
27. Wegen S, Roth KS, Weindler J, Claus K, Linde P, et al. 2023. First clinical experience with [$^{68}$Ga] Ga-FAPI-46-PET/CT versus [$^{18}$F] F-FDG PET/CT for nodal staging in cervical cancer. *Clin Nucl Med* 48(2): 150-155. https://doi.org/10.1097/RLU.0000000000004505
28. Kratochwil C, Flechsig P, Lindner T, Abderrahim L, Altmann A, et al. 2019. $^{68}$Ga-FAPI PET/CT: tracer uptake in 28 different kinds of cancer. *J Nucl Med* 60(6): 801-805. https://doi.org/10.2967/jnumed.119.227967
29. Gege Z, Xueju W, Bin J. 2023. Head-to-head comparison of $^{68}$Ga-FAPI PET/CT and FDG PET/CT for the detection of peritoneal metastases: systematic review and meta-analysis. *Am J Roentgenol* 220(4): 490-498. https://doi.org/10.2214/AJR.22.28402
30. Viergever BJ, Raats DA, Geurts V, Mullenders J, Jonges TN, et al. 2024. Urine-derived bladder cancer organoids (urinoids) as a tool for cancer longitudinal response monitoring and therapy adaptation. *Br J Cancer* 130(3): 369-379. https://doi.org/10.1038/s41416-023-02494-6
31. Sjödahl G, Lauss M, Lövgren K, Chebil G, Gudjonsson S, et al. 2012. A molecular taxonomy for urothelial carcinoma. *Clin Cancer Res* 18(12): 3377-3386. https://doi.org/10.1158/1078-0432.CCR-12-0077-T
32. Naganawa S, Yoshikawa T, Yasaka K, Maeda E, Hayashi N, et al. 2017. Role of delayed-time-point imaging during abdominal and pelvic cancer screening using FDG-PET/CT in the general population. *Medicine* 96(46): e8832. https://doi.org/10.1097/MD.0000000000008832